PowderMet 2008, 2008-01-0396
SAND2008-4277C

SYNTHESIS AND CHARACTERIZATION OF HYBRID AL/AL$_3$NI FOAM MATERIALS VIA LENS® DEPOSITION OF NI-COATED AL POWDER

Baolong Zheng[1], John E. Smugeresky[2], Yizhang Zhou[1], Dean Baker[3], Asit Biswas[3], and Enrique J. Lavernia[1]

[1]Department of Chemical Engineering and Materials Science
University of California, Davis, CA 95616
[2]Sandia National Laboratories, Livermore, CA 94551-0969
[3]Advanced Powder Solutions, Inc., Cypress, TX 77095

ABSTRACT

In this study, Laser Engineered Net-shaping (LENS®) technique was used to synthesize hybrid Al/Al_3Ni foam materials from Ni-coated 6061 Al powder. During LENS® processing, Ni reacted with the Al matrix, leading to the formation of an intermetallic compound, Al_3Ni, which can effectively behave as a reinforcement phase, while a high volume of pores (up to 60%) was formed in-situ. The microstructure of the as-deposited Al/Al_3Ni foams was characterized using SEM, EDS, and XRD techniques. The microstructural evolution, including intermetallic compound Al3Ni formation, and porosity variation was analyzed on the basis of the thermal field that was present during deposition. The mechanical response of the as-deposited material was characterized using compression and hardness testing, indicating that the strength and hardness are 190 MPa and 320 HV, respectively.

1. INTRODUCTION

Cellular metallic foams have engendered technical interest as a result of their unique physical and mechanical properties, such as high stiffness in conjunction with very low specific weight, and hence their ability to absorb energy [1-12]. The potential applications of cellular metallic foams include cushioning, insulating, damping, construction, biomedical implants, and filtering purposes, to provide some obvious examples [13]. In the particular case of Al based foams, applications of relevance include lightweight structures for the automotive, aerospace, and allied industries [2, 5-8, 10, 14-16]. In addition, advances in the near net shaping of aluminum foam have expanded in the realm of potential structural applications.

In general, foamed Al does not have sufficient strength for some commercial applications. Various strengthening and toughening approaches have been explored, including grain boundary strengthening, solid solution strengthening, precipitation strengthening, and particulate reinforcement. Several of them, such as solid solution strengthening and ceramic reinforcement, have been suggested to improve the strength characteristics of foamed Al alloys [17-19]. Introduction of particulate reinforcements, for example, is considered to be a effective approach to increasing the strength and toughness of Al alloys, and has furthermore, led to the development of new types of Al metallic foam materials. Intermetallic compounds, due to their high strength, and can be considered candidate reinforcement particles in the ductile Al alloy matrix. `

Various methods including casting and powder metallurgy (PM) techniques have been successfully used in conventional manufacturing of metallic foams via conventional melting and molding processes [2, 3], which generally require addition of foaming agents for the formation of pores. In the present paper, an alternative process of Laser Engineered Net Shaping (LENS®) using a laser as a heat source is introduced. The LENS® process is a laser-assisted, direct metal manufacturing process that provides a pathway to produce net shaped components [20, 21]. The LENS® process incorporates features from stereo-lithography and laser cladding, using computer-aided design (CAD) files to control the forming process. Powder is delivered in a carrying gas stream through four nozzles that converge at the same point on the focused Nd:YAG laser beam to form a molten pool, and a three-dimensional part can be generated line by line and layer by layer via additive processing. The primary advantages associated with LENS® process are: small heat affected zone (HAZ) with high cooling rate resulting in a fine microstructure; easy gradient deposition of multiple materials within a single component; and fully dense near-net shape metal components. Reductions in time, energy and cost to build net shaped parts are also expected over conventional casting and powder metallurgy techniques. Cooling of the melt depends on LENS® processing parameters, such as laser input energy, substrate (or laser) traverse speed, powder feeding rate, and substrate temperature [22, 23]. This flexibility may empower the control of the pore formation, microstructure and properties of the LENS® deposited components.

In the present study, the potential of the LENS® process to fabricate hybrid Al based foam materials containing dispersed Al_3Ni intermetallic particles, from Ni coated Al6061 powder without the addition of a foaming agent was evaluated. The anticipated benefits of the proposed approach include: enhanced strength from the in-situ formed Al_3Ni phase and a low density from formation of high amount of pores. The microstructures of the LENS® deposited hybrid Al foam were characterized using scanning electron microscopy (SEM), X-ray energy-dispersive spectroscopy (EDS) analysis, and X-ray diffraction (XRD). Efforts were also devoted to analysis of the pore formation, microstructural and mechanical characterization of the LENS® deposited hybrid Al based foam. The compressive mechanical properties of the LENS® deposited Al based foam were studied, in combination with the analysis of LENS® processing.

2. EXPERIMENTS

The powders used in the present study were 15-20wt.%Ni-coated Al6061 powder, with a size range of 45-120 μm, provided by Advanced Powder Solutions, Inc. (Cypress, TX). The experiments were performed with a 750 LENS® system (Optomec, Inc. Albuquerque, NM) which consists of a continuous wave (CW) mode Nd:YAG laser operating up to 650 W at 1064 nm, a four-nozzle coaxial powder feed system, a controlled environment glove box, a motion control system, and real-time molten pool sensor (MPS) and Z-height control (ZHC) subsystem [24] as shown in Figure 1. Compared to CO_2-laser radiation, aluminum exhibits higher absorption to Nd:YAG laser used in LENS® processing [25].

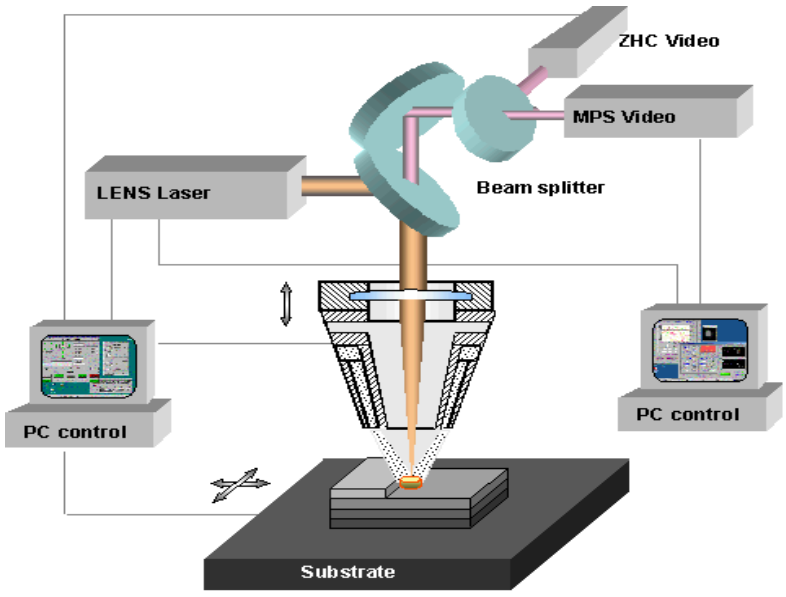

Fig. 1. Schematic of LENS® process equipped with molten pool sensor and Z-height control system.

Cuboidal block samples of 10 mm x 10 mm x 20 mm were fabricated. Successive layers were deposited with the hatch lines of two adjacent layers at an angle of 90°. The hatch space is 0.38 mm, delta Z is 0.25 mm, laser output power is 250 W, traverse speed is 17 mm/s, and the powder feed rate is 10 rpm. The entire process was carried out in Ar environment to avoid oxidation during deposition. The oxygen level in the glove box was maintained below 10 ppm during deposition.

Mechanical testing was conducted at ambient temperature with an Instron 8801 apparatus. The test specimens were electrodischarge-machined (EDM), producing cubic specimens (4 mm x 4 mm x 4 mm) for the compressive test. Prior to testing, the surfaces of all EDM specimens were polished to remove any oxide layers present. The cross-section microstructure of the fabricated Al foam samples was observed with optical microscopy (OM) and SEM. XRD with CuK-α radiation was used for microstructure and phase analysis.

3. RESULTS AND ANALYSIS

3.1. CHARACTERISTICS OF NI-COATED Al POWDER

Figures 2 and 3 show the SEM (BSE) micrographs and the EDX mapping of Ni-coated Al 6061 powder particles, respectively. It can be seen that the atomized Al6061 powder particles are completely covered by the Ni coating with a uniform thickness of about 1 μm. TEM observation [26] indicated that there is no presence of micro-scale faults, such as voids and cracks, at the interface between Ni coating and the core. It is worth noting that previous TEM examination showed that the coating comprises single phase, nearly equiaxed grains with size from 10 to 100 nm, indicating that the Ni coating is nano-crystalline [26]. The presence of a nano-structure in the coating can be rationalized on the basis of a rapid quenching mechanism during cooling from the liquid state. It has been argued that rapid displacement of the liquid/solid interface will lead to an equiaxed structure with nanoscale dimensions, due to limited growth time during rapid solidification [27, 28]. The Al6061 core and the Ni coating appear to be well bonded, based on these limited observations.

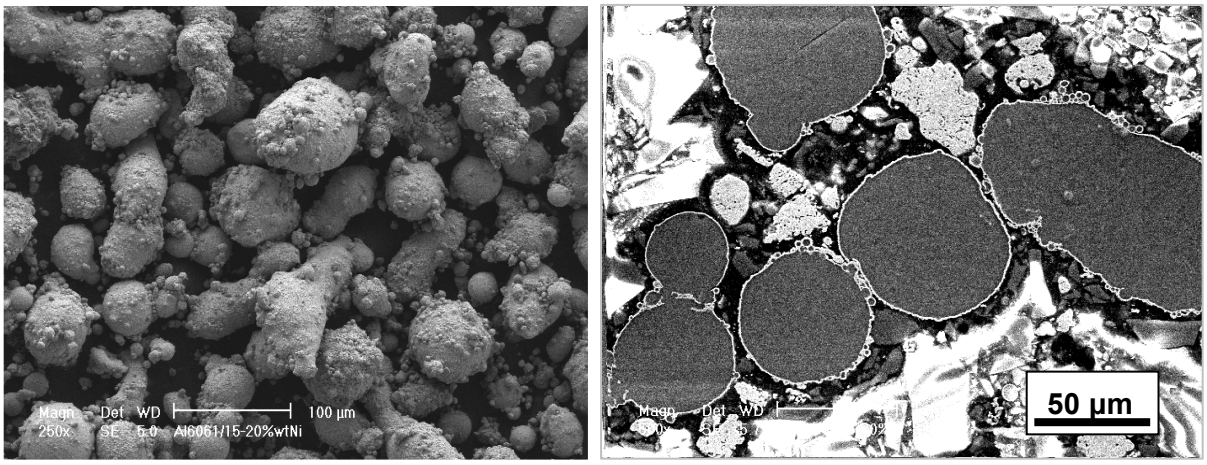

(a) (b)

Fig. 2. SEM morphology of Ni coated Al6061 particles.

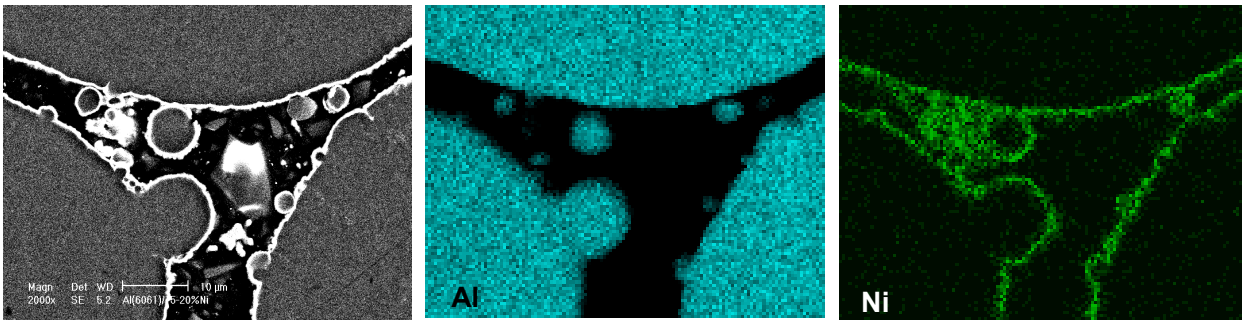

Fig. 3. EDS mapping of Ni coated Al6061 particles.

3.2. MICROSTRUCTURE OF DEPOSITED Al FOAM

For the microscopic observation and porosity measurement, the foamed Al-blocks were cross-sectioned, following by grinding and a fine final polishing using the conventional techniques, modified to take into account the porosity and possible metal smearing that would alter the fractional porosity measurements. Figure 4 shows the (a) OM and (b) SEM micrographs of the LENS® deposited hybrid Al based foam. It is evident that a high volume fraction of porosity and rather large average pore sizes formed in the deposited Al materials. The microstructure suggests that the Ni coating on the Al-6061 particles surface melted during deposition. EDS mapping results indicated that the lighter phases (in Figure 4b) are rich of Ni. Furthermore, the Ni reacted with Al, leading to the formation of Al-Ni (Al_3Ni) intermetallic compounds (lighter gray phase in the Figure 4(b)), which can act as a reinforcement phase, while a high volume of pores were formed and uniformly dispersed in the darker Al matrix for weight reduction. Most of pores exhibit a closed cell structure. This volume fraction and average pore size are not typical of LENS deposited materials. However, the spherical and closed porosity could lead to a high degree of energy absorption and possible use of the material.

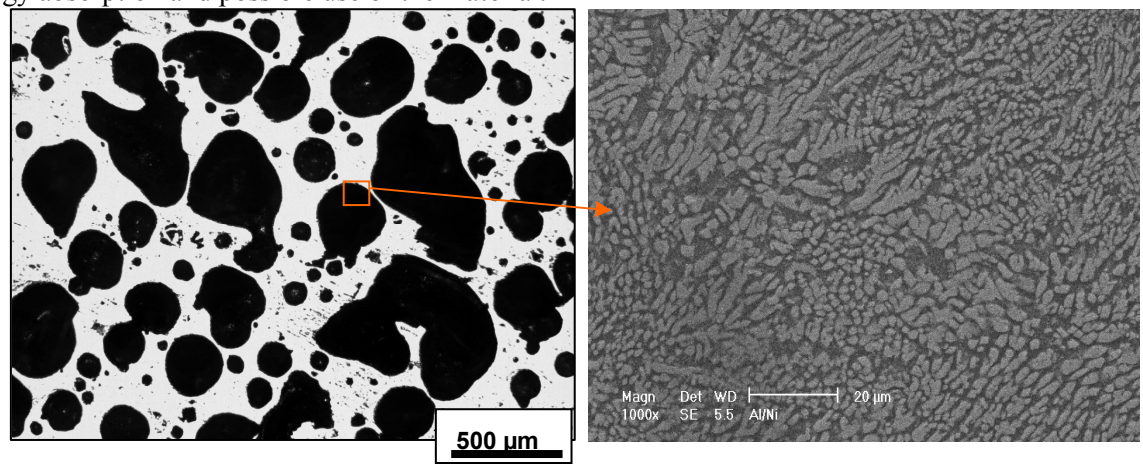

(a) (b)

Fig. 4. Micrograph of LENS® deposited Al+Al_3Ni foam materials showing (a) high volume of pores, and (b) intermetallic compound (gray) in Al matrix (dark).

There are several mechanisms by which the porosity can form. The porosity formation can be attributed to gas in the starting powders [29] that was generated and further entrapped in the melt during LENS® deposition. The pores could also come from the vaporizing/ expansion of the low boiling point (2060°C) Al phase in the core of Ni coated Al particles, while outside high boiling point (3175°C) Ni coating and reacted Ni-Al phases are still in the molten state. There are also other less likely possible sources, for formation of fine pores, such as pores caused by the collapse of unstable keyholes [30, 31], pores due to entrapment of gases by surface turbulence, gas entrainment during turbulent impact of particles into the molten pool, contamination by powder-feed gases, moisture absorbed on powder surfaces [32], and shrinkage porosity [33, 34]. Moreover, the porosity arising from reaction synthesized Al-Ni could evolve from gaseous phases produced during the reaction at high temperature, Kirkendall porosity generated due to unbalanced diffusivity between Ni and Al when solid-state inter-diffusion occurs prior to

reaction [35], and intrinsic porosity due to the volume change between products Al_3Ni and reactants of Al and Ni. Those porosity sources hinder a straightforward explanation in many cases [29, 36-39]. The higher melt viscosity resulting from the presence of large quantity of primary Al_3Ni phases could restrict the release of gas from melt.

Porosity evaluation was conducted using standard image analysis software AnalySIS 3.1. For each image the area covered by all pores was detected as dark area as shown in Figure 4(a). The results of all images were summarized in tables for statistical analysis. Figure 5 shows the variation of mean porosity value for each field with position in the deposited Al foam. It is found that the fraction of porosity can reach up to 60%. The fraction of porosity is higher in middle area than that in bottom, top and side edge area of the deposited component.

This strong variation in the pore size as a function of spatial location in the deposits may depend upon the processing parameters in the following way. At higher processing speed, the pore size is relatively fine due to a short beam interaction time. Microscopically, besides a temperature gradient in the molten pool, there is also a gradient of molten liquid pressure, which could result in the bubble expansion as it moves from bottom to the top surface of the molten pool. However, this does not explain the systematic variation in the size of the pores from the bottom to the top of deposit that was observed.

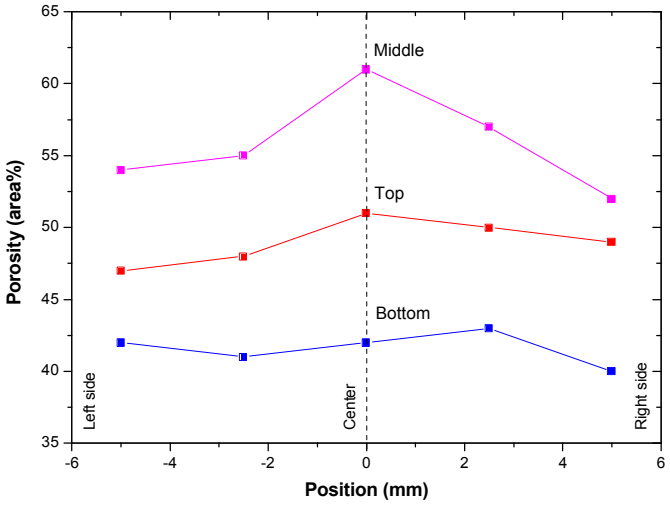

Fig. 5. Porosity varies by position along cross-section of deposited Al foam.

However, consider rationalizing the data in Figure 5 based on the thermal evolution of the deposited material during processing. At the start of the deposition stage, the cold substrate leads to high cooling and solidification conditions. Rapid solidification will hinder pore nucleation and growth, resulting in low porosity in the bottom region. This effect is similar to the case of fast processing speed that is short interaction time, which also leads to a high cooling rate. The temperature monotonically increases with deposited material thickness because the accumulation of thermal energy at the end of each cycle

causes the temperature to be somewhat higher than that at the end of its previous cycle. With increasing deposition height the temperature of the melt pool increases and reaches a value that is sufficient to maintain a liquid phase. As the viscosity of melt decreases with increasing temperature, the bubbles can readily aggregate and be release from the melt. As a result, the volume fraction of porosity decreases at the top region of the deposit. This release of the pores could occur when the laser beam interaction time becomes considerably long, due to superheating of the molten pool. So, if we consider the conditions that are present during the deposition of the middle region as optimized processing conditions for the foaming to occur, we have identified overall conditions that are beneficial for pore formation and growth, and conclude that the melt foaming is completed before the pores can collapse and/or be released from the melt.

It appears that during deposition, molten Al and Ni react, resulting in the in-situ formation of an Al-Ni intermetallic compound. If the Al intermetallic compound is Al_3Ni, it is good in resistance for wear, high hardness and stability at an elevated temperature, but brittle and cannot serve as a structural material alone. However, this phase does have high strength, and could act as reinforcement for the Al alloy. The brittleness of the intermetallic compound could be compensated if it is embedded in the ductile aluminum alloy matrix. Thus, the advantageous properties of Al–Al_3Ni composite can be utilized in a structural material and the ductility of matrix material Al can assure that the material as whole is not brittle. The microstructure observed in Figure 4b suggests that the benefits from a dispersed Al_3Ni in an aluminum matrix to obtain high strength and formation of large amount of porosity to obtain a low density were realized. Whether this is in fact attributed to the heat released by the exothermal reaction between Al and Ni, is not clear, but certainly it can account for temperature excursion higher than those expected from laser heating alone.

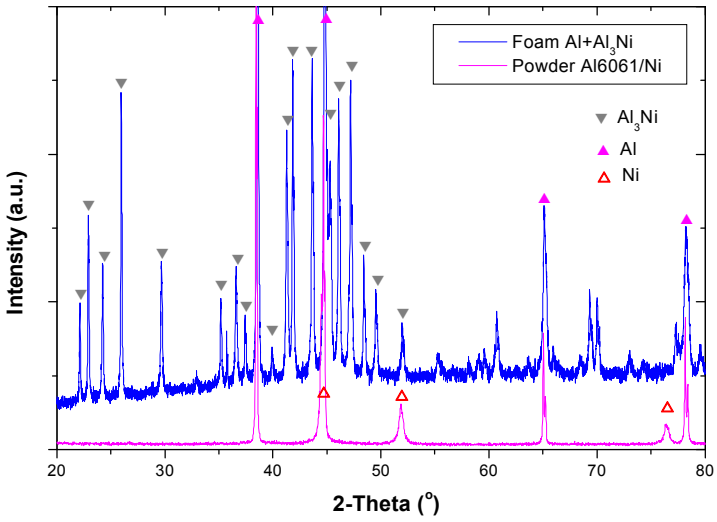

Fig. 6. XRD patterns of LENS®deposited Al based foam and powder used indicating formation of Al_3Ni.

Figure 6 presents the XRD patterns of the LENS® deposited Al based foam and Ni-coated Al6061 powder, respectively. The XRD analysis indicated that LENS® deposited Al based foam is two phased, containing only Al and Al_3Ni. Please note that the peaks of Ni were not detected in the foam materials. This means that the nickel dissolved into the aluminum, but precipitated out as Al_3Ni in a pure Al matrix (see Phase diagram). In the case of the XRD results from Ni-coated Al6061 powder, the peaks only corresponding to both Al and Ni were detected, showing no reaction at the interface between Al and Ni coating during the coating process.

3.3. MECHANICAL PROPERTIES

The mechanical properties of metallic foams depend on fraction of theoretical density, pore size, structure and size distribution. The micro-hardness as a function of distance from the substrate is shown in Figure 7. The micro-hardness is highest for the first layer, and decreases with increasing distance from the substrate. Experimental and numerical results [40, 41] suggest this is due to the decreasing of cooling rate with distance form the substrate. After an initial temperature peak, heat is quickly dissipated away and the initial thermal transient leads to a rapid quenching effect in the first few layers with cooling rate decreasing with distance from the substrate. Higher cooling rates correspond here to a harder material, lower cooling rates to a softer material. Assuming that higher cooling rates result in finer grain size/microstructure, the hardness can be attributed to grain size strengthening. Since the cooling rate is also inversely proportional to the laser power level used in the experiments, the higher quench rates are available at the lower laser power output when a smaller molten pool size is realized and the grain size is expected to be smaller. Lower quench rates occurring when higher laser power output is used, allows for a larger melt pool size and time for grain growth to occur and a lower micro-hardness is expected.

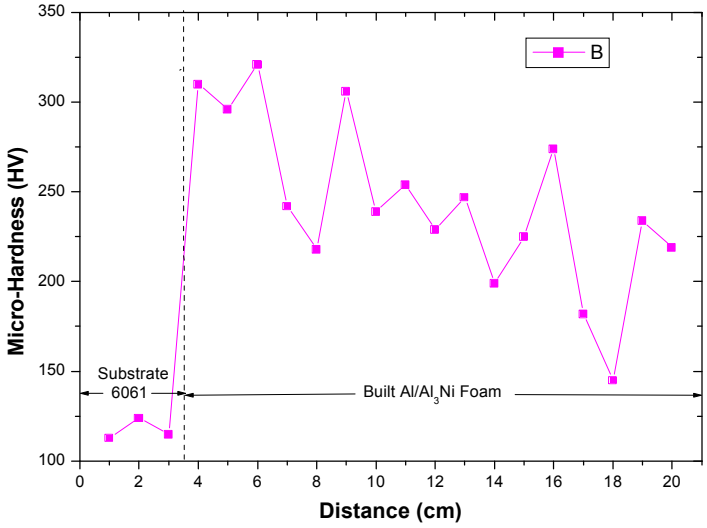

Fig. 7. Variation of micro-harness of LENS® deposited hybrid Al based foam with distance from the substrate.

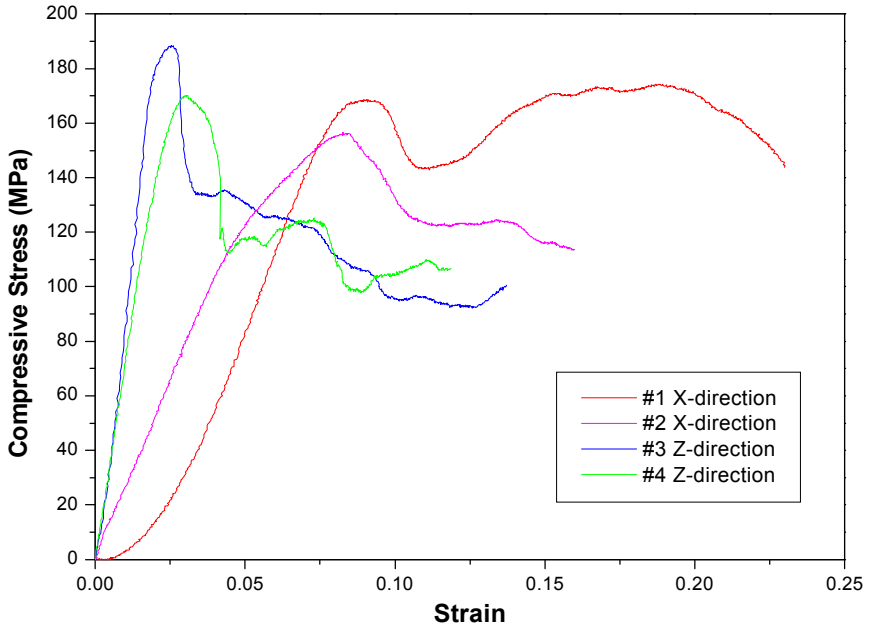

Fig. 8. Compressive test result of LENS® deposited Al+Al_3Ni foams.

Mechanical tests were conducted primarily in compression at room temperature under quasi-steady loading rates (0.001 mm/s). Figure 8 shows the uniaxial compressive testing stress-strain results performed on cuboid specimens of LENS® deposited hybrid Al based foam with different compressive directions. Compressive testing direction is in either parallel (Z) or perpendicular (X) to the deposition build direction. The results showed that the yield strength of LENS® deposited hybrid Al based foam can reach to 190 MPa, while the yield strength of the wrought Al6061 alloy is 48 MPa for annealed and 131 MPa for T4 tempered [42]. The measured density of LENS® deposited hybrid Al based foam is 2.0 g/cm^3, while the density of the wrought Al6061 alloy is 2.7 g/cm^3. The testing results with different compressive directions showed different strain-stress curves, indicating the microstructure of the fabricated foams is anisotropic. The fact that elastic modulus and yield strength in build direction (Z) is higher than that in the plane of the layers (X) might be owing to most of heat transferred to substrate in Z-direction, and grain growth tend to follow heat transfer direction.

The characteristics of flow stress (Figure 8) exhibits a variation of about 20% among the 4 specimens. The variation of stress after yield is due to collapse of the pores and localized fracture of matrix. The sequence of deformation events observed was elastic deflection of the cell element, followed by localized deformation in a few cells [43], formation of a deformation band [17], collapse and densification of cells within this bend, and gradual spreading of this band through the entire sample. The initial response reflects the elastic deformation of cell elements and is followed by localized yielding.

4. SUMMARY

Our preliminary results here indicate that the feasibility of fabricating in-situ hybrid Al+Al3Ni metallic foam components via LENS® process has been demonstrated without the need for a foaming agent. The volume fraction of closed pores obtained in the present study ranged from 40 to 60%. The LENS® deposited hybrid Al+Al_3Ni metallic foams showed higher strength as compared to its monolithic matrix alloy Al6061, and a significant lower density of 2.0 g/cm^3. During LENS® processing, Ni coating reacted with Al matrix alloy powders, which contributed to pore formation. The reaction product of Al_3Ni intermetallic compound was uniformly dispersed in Al matrix, presumably contributing to the mechanical response as a reinforcement phase. Changes in pore structure, wall material and microstructure influence yielding behavior and the subsequent collapse mechanism of the cell elements. The advantages of LENS® processing hybrid Al+Al_3Ni metallic foams include localized processing, the control foam characteristics through LENS® process parameters, and no need for a foaming or pore forming agent.

ACKNOWLEDGMENTS

Work at UC Davis and APS is supported by NASA STTR Contract NNM06AB11C. Work by Sandia National Laboratories is supported by the U. S. DOE under contract DE-AC04-94AL85000. Sandia is a multi-program laboratory operated by Sandia Corporation, a Lockheed Martin Company, for the United States Department of Energy.

REFERENCE

[1] A. H. Brothers, D. C. Dunand, Scripta Materialia 54 (2006) 513-520.
[2] J. Banhart, Progress in Materials Science 46 (2001) 559-632.
[3] G.J. DAVIES, S. ZHEN*, JOURNAL OF MATERIALS SCIENCE 18 (1983) 1899--1911.
[4] A. Bansiddhi, T. D. Sargeant, S. I. Stupp, D. C. Dunand, Acta Biomaterialia In Press, Corrected Proof.
[5] S. Esmaeelzadeh, A. Simchi, Materials Letters 62 (2008) 1561-1564.
[6] Y. P. Jeon, C. G. Kang, S. M. Lee, Journal of Materials Processing Technology In Press, Corrected Proof (2008).
[7] K. Lemster, M. Delporte, T. Graule, J. Kuebler, Ceramics International 33 (2007) 1179-1185.
[8] G. Lu, J. Shen, W. Hou, D. Ruan, L. S. Ong, International Journal of Mechanical Sciences 50 (2008) 932-943.
[9] B. P. Neville, A. Rabiei, Materials & Design 29 (2008) 388-396.
[10] R. E. Raj, B. S. S. Daniel, Journal of Alloys and Compounds In Press, Corrected Proof.
[11] P. Sevilla, C. Aparicio, J. A. Planell, F. J. Gil, Journal of Alloys and Compounds 439 (2007) 67-73.
[12] H. Shen, S. M. Oppenheimer, D. C. Dunand, L. C. Brinson, Mechanics of Materials 38 (2006) 933-944.
[13] AMS Handbook, Metal powder production and characteization, 7 (1998) 1043-1047.
[14] L. Peroni, M. Avalle, M. Peroni, International Journal of Impact Engineering 35 (2008) 644-658.

[15] A. Pollien, Y. Conde, L. Pambaguian, A. Mortensen, Materials Science and Engineering: A 404 (2005) 9-18.
[16] Y. P. Kathuria, Surface and Coatings Technology 142-144 (2001) 56-60.
[17] O. Prakash, H. Sang, J. D. Embury, Materials Science and Engineering A 199 (1995) 195-203.
[18] S. Yu, Y. Luo, J. Liu, Materials Science and Engineering: A In Press, Corrected Proof.
[19] W. Jiejun, L. Chenggong, W. Dianbin, G. Manchang, Composites Science and Technology 63 (2003) 569-574.
[20] C. L. Atwood, M. L. Griffith, L. D. Harwell, D. L. Greene, D. E. Reckaway, M. T. Ensz, D. M. Keicher, M. E. Schlienger, J. A. Romero, M. S. Oliver, F. P. Jeantette, J. E. Smugeresky, Sandia Report SAND99-0739, Sandia National Laboratories (1999).
[21] B. Zheng, Y. Xiong, J. Nguyen, J. E. Smugeresky, Y. Zhou, E. J. Lavernia, J. M. Schoenung, Powder Additive Processing with Laser Engineered Net Shaping (LENS), in: F. Columbus (Ed.) Powder Metallurgy Research Trends, Nova Science Publishers, Inc, Hauppauge, NY, 2008.
[22] B. Zheng, J. E. Smugeresky, Y. Zhou, D. Baker, E. J. Lavernia, Metallurgical and Materials Transactions A, (2008) Accepted.
[23] W. Hofmeister, M. Griffith, M. Ensz, J. Smugeresky, JOM (2001) 30-34.
[24] J. E. Smugeresky, B. Zheng, L. Ajdelsztajn, Y. Zhou, J. M. Schoenung, E. J. Lavernia, 134th TMS Annual Meeting & Exhibition, San Francisco, CA, Feb. 13-17, 2005 (2005).
[25] J. F. Ready, D. F. Farson, LIA Handbook of Laser Materials Processing, Laser Institute America, Magnolia Publishing, Orlando, FL, 2001.
[26] J. He, Y. Zhou, D. Baker, W. Harrigan, E.J. Lavernia, Ceramic powder encapsulated by nanocrystalline metallic coating, in: MS&T 2003, , Chicago, IL, , 2003, pp. 167-172.
[27] E.J. Lavernia, J. D. Ayers, a. T. S. Srivatsan, Int. Mater. Rev. 37 (1992) 1-44.
[28] Dieter M. Herlach, Materials Science and Engineering R12, 4-5 (1994) 177-272.
[29] D. F. Susan, J. D. Puskar, J. A. Brooks, C. V. Robino, Materials Characterization 57 (2006) 36-43.
[30] M. Pastor, H. Zhao, T. DebRoy, J. Laser Appl. 12 (2000) 91~100.
[31] E. Aghion, B. Bronfin, Mater. Sci. Forum 350-351 (2000) 19~28.
[32] J. Wegrzyn, M. Mazur, A. Szymanski, B. Balcerowska, Weld. Int. 2 (1987) 146~150.
[33] X. Cao, W. Wallace, J.P. Immarigeon, C. Poon, Mater. Manufact. Process. 18 (2003) 23~49.
[34] X. Cao, W. Wallace, C. Poon, J.P. Immarigeon, Mater. Manufact. Process. 18 (2003) 1~22.
[35] K. Morsi, Materials Science and Engineering A 299 (2001) 1-15.
[36] P. A. Kobryn, E. H. Moore, S. L. Semiatin, Scripta Materialia 43 (2000) 299-305.
[37] G. K. Lewis, E. Schlienger, Materials & Design 21 (2000) 417-423.
[38] B. Zheng, J. E. Smugeresky, Y. Zhou, E. J. Lavernia, Advances in Powder Metallurgy & Particulate Materials--2006, Proceeding of the PowderMet 2006 (2006) 10/81-94.
[39] Y. Xiong, B. Zheng, J. E. Smugeresky, L. Ajdelsztajn, J. M. Schoenung, MS&T'05 Pittsburgh, PA, USA, 09/25-28/2005 (2005).
[40] B. Zheng, Y. Zhou, J. E. Smugeresky, J. M. Schoenung, E. J. Lavernia, Part I Numerical Calculations, Metallurgical and Materials Transaction A, (2008) Accepted.
[41] B. Zheng, Y. Zhou, J. E. Smugeresky, J. M. Schoenung, E. J. Lavernia, Part II Experimental Investigation and Discussion, Metallurgical and Materials Transaction A, (2008) Accepted.

[42] ASM Handbook, Properties and Selection: Nonferrous Alloys and Special-Purpose Materials Vol.02 (1992) 102-103.
[43] Y. Sugimura, J. Meyer, M. Y. He, H. Bart-Smith, J. Grenstedt, A. G. Evans, Acta Materialia 45 (1997) 5245-5259.